

See discussions, stats, and author profiles for this publication at: <https://www.researchgate.net/publication/6534465>

Reversible, Erasable, and Rewritable Nanorecording on an H₂ Rotaxane Thin Film

ARTICLE in JOURNAL OF THE AMERICAN CHEMICAL SOCIETY · MARCH 2007

Impact Factor: 12.11 · DOI: 10.1021/ja067037p · Source: PubMed

CITATIONS

48

READS

67

10 AUTHORS, INCLUDING:



Li Gao

California State University, Northridge

45 PUBLICATIONS 887 CITATIONS

SEE PROFILE



Shixuan Du

Chinese Academy of Sciences

133 PUBLICATIONS 2,397 CITATIONS

SEE PROFILE



Dong-Xia Shi

Chinese Academy of Sciences

107 PUBLICATIONS 2,499 CITATIONS

SEE PROFILE



Hongjun Gao

Chinese Academy of Sciences

150 PUBLICATIONS 3,771 CITATIONS

SEE PROFILE

Reversible, Erasable, and Rewritable Nanorecording on an H2 Rotaxane Thin Film

Min Feng,[†] Li Gao,[†] Zhitao Deng,[†] Wei Ji,[†] Xuefeng Guo,[‡] Shixuan Du,[†] Dongxia Shi,[†] Deqing Zhang,[‡] Daoben Zhu,[‡] and Hongjun Gao^{*,†}

Institute of Physics and Institute of Chemistry, Chinese Academy of Sciences, Beijing 100080, China

Received October 9, 2006; E-mail: hjgao@aphy.iphy.ac.cn

Reversible, erasable, and rewritable nanoscale recording on organic thin films is of practical importance in ultrahigh density information storage. The scanning tunneling microscope (STM) is a powerful tool that enables nanorecording on organic films by inducing conductance transitions of the organic molecules.^{1–6} Rotaxane molecules have shown significant potential to be used as the building blocks for molecular electronics.^{7,8} Writing high-conductance nanoscale marks on rotaxane H1 thin films was realized using STM in our previous studies, while, erasing of the marks showed some difficulties.⁹ In this Communication, we report on the reversible, erasable, and rewritable nanorecording on the rotaxane H2 Langmuir–Blodgett (LB) thin films. The dots written with ~ 3 nm feature size show significant stability in air at room temperature.

Figure 1a shows the structure of the H2 molecule. It is a variation of the H1 molecule.¹⁰ An H2 molecule consists of a π -electron-deficient ring cyclobis(paraquat-*p*-phenylene) (CBPQT⁴⁺) and a dumbbell-shaped component. The dumbbell component has two π -electron-rich recognition sites (TTF and DNP; see Figure 1a) and is terminated by bulky “stoppers”. The ring encircles part of the dumbbell, making them mechanically interlocked with each other. The ring can move back and forth between the two different π -electron-rich recognition sites in response to the external stimuli, resulting in the switching between the two stable structures. Recent theoretical calculations^{11–13} have revealed that the movement of the CBPQT⁴⁺ ring is accompanied by a change in molecular electronic structure. The difference between H1 and H2 molecules lies in the spacer between TTF and DNP. In H2, a rigid cyclohexyl spacer replaces the soft alkyl spacer ($-(\text{CH}_2)_5-$) in H1.¹⁰

For STM recording, the H2 rotaxane thin films with ~ 20 nm thickness were prepared on highly oriented pyrolytic graphite (HOPG) substrates using the LB technique; For macroscopic I–V characterization, the films with a thickness of ~ 70 nm were prepared on the indium tin oxide (ITO) coated glass substrates; And for the micro-Raman studies, the thin films were also prepared on ITO coated glass substrates. The thickness of the film is about 100 nm, with some protuberant islands of ~ 400 nm in height. The micro-Raman spectra were acquired on these plateaus with an excitation wavelength of 632.8 nm.

By applying voltage pulses onto the H2 thin films through the STM tip, we realized the repeatable and rewritable nanorecording (Figure 1b). Nanoscale dots can be written repeatedly with the voltage pulses (~ 2.0 V, 0.1–10 ms). This case is similar to that of the H1 thin films.⁹ What is more interesting is that the marks written on the H2 thin films can be erased, re-recorded, and re-erased on the same site. In the whole recording process, the dots remain a size of ~ 3 nm and are stable in air at room temperature for more than 12 h. The marks are directly visible in the current image in

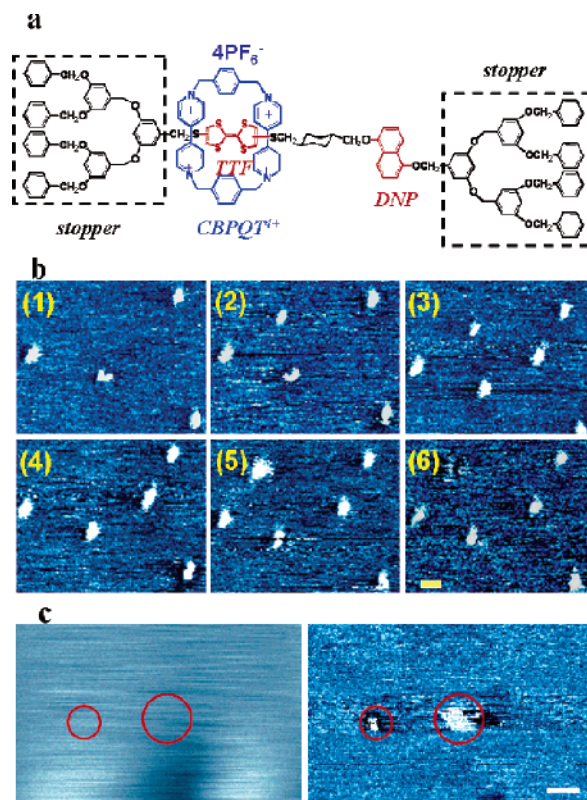


Figure 1. (a) Molecular structure of the H2 molecule. (b) Frames 1–3 show bright marks written one by one using STM; frames 4–6 show the erasing, rewriting, and re-erasing on the same recording site, with $V_b = 0.8$ V, $I_t = 0.05$ nA. The voltage pulse for recording was 2 V for 3 ms, the pulse for erasing was -2 V for 3 ms. Scale bar is 6 nm. (c) Topographic (left) and current (right) AFM images of two marks written by conductive contact AFM on a 8 nm thick H2 films. Scale bar is 10 nm.

conductive contact AFM characterizations, but invisible in the topographic image [see Figure 1c], suggesting that appearance of dots are indeed due to conductance transitions of the H2 molecules. Our further studies show that the H2 films are competent for the reversible nanorecording even after 1 month of being stored in air at room temperature.

To verify the origin of the conductance transitions of the H2 molecules, we performed the macroscopic I–V measurements on the H2 films using a standard I–V characterization system (Keithley, model 4200SCS). The ITO substrate served as one electrode. We used a freshly cleaved HOPG plate as another electrode, which was pressed against the H2 thin film to ensure a good contact. Figure 2 shows the I–V characteristic of the H2 film, which manifests an electrical bi-stability with a threshold of 1.4 V. The film is initially in the high-impedance state of $10^8 \Omega \cdot \text{cm}$, while at 1.4 V, the film abruptly switches to a low-impedance

[†] Institute of Physics.[‡] Institute of Chemistry.

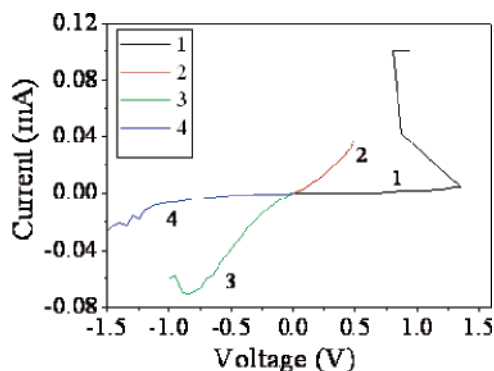


Figure 2. Current–voltage relations on the same region of an H2 thin film showing the reversible conductance transition with applied voltages. (curve 1) When initially applying the voltage from 0 to 1.4 V, I–V curve shows the transition from high to low impedance. (curve 2) The film retains the low impedance state when applying the voltage from 0 to 0.5 V. (curve 3) When a negative voltage from 0 to -1.0 V is applied, the film retains the low impedance state at first, but begins to recover the original high impedance state at -1.0 V. (curve 4) A negative voltage from 0 to -1.5 V is applied, and the conductance is now at the original high impedance level.

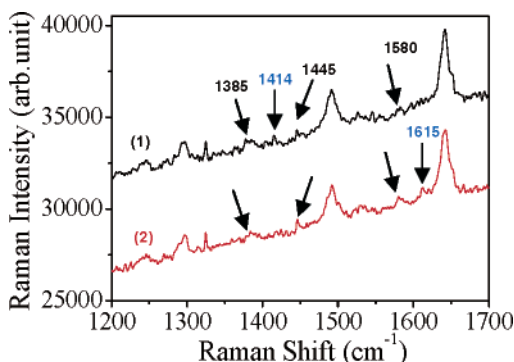


Figure 3. Raman spectra of the H2 rotaxane thin film before (1) and after (2) the conductance transition.

(conductive) state of $10^6 \Omega \cdot \text{cm}$ (curve 1 in Figure 2). A subsequent voltage scan from 0 to 0.5 V (curve 2) on the same region verifies that the H2 thin film keeps the new state of low-impedance, exhibiting a memory effect. When a reverse voltage is applied, the film returns to its original insulating state (curve 3 and 4). The conductance difference between the two states is 2 orders of magnitude. Our extensive measurements showed that this conductance transition can be well repeated. No obvious degradation of the thin film was observed after 6 cycles. These results indicate that the H2 film possesses the reversible conductance transition properties controlled by the external voltages.

Theoretical studies^{11–13} have demonstrated that the conductance switching of the rotaxane molecules is induced by the movement of the CBPQT⁴⁺ between TTF and DNP recognition sites. Micro-Raman spectra of the H2 film, acquired before and after the conductance transition from insulating to conductive states, show distinct changes in two regions, $1385\text{--}1445 \text{ cm}^{-1}$ and $1580\text{--}1640 \text{ cm}^{-1}$ [see Figure 3]. Our density functional calculations reveal that the peak at 1414 cm^{-1} originates from the shared C=C torsional vibration of DNP. The disappearance of 1414 cm^{-1} peak in the conductive state might be a result of the depressed C=C torsional vibration of DNP when CBPQT⁴⁺ moves to it, while a new peak located at 1615 cm^{-1} appears after the conductance transition,

ascribed to the C=C stretching vibration of TTF group when the CBPQT⁴⁺ leaves. On the basis of the experimental and theoretical results, we suggest that the conductance transition of the H2 thin film originates from the intramolecular motion of CBPQT⁴⁺.

We suggest that the spacers in the molecules might be responsible for the different behaviors of nanorecording erasable in the H2 thin film, not in the H1 thin film. The alkyl chain is relatively soft and the steric hindrance is relatively small compared to the cyclohexyl group. It is likely that two H1 molecules are packed very close with a layout of (TTF–DNP–space)/(space–TTF–DNP). When the ring moves from TTF to DNP, the TTF group in adjacent H1 molecules may stabilize the overall system. This will make it difficult for the ring to move back to TTF site, and consequentially, the nanoscale dots in the H1 thin films are difficult to erase. In contrast, the spacer in H2 molecule is relatively rigid, and correspondingly, the intermolecular interaction of H2 molecules will not be as strong as that in H1 molecules. This makes the CBPQT⁴⁺ ring move back to the TTF from DNP sites less toilsomely. Therefore, the relaxation of the ring from metastable state to the ground state is enhanced, which makes it possible for the recovery of the original state in the H2 molecules, and consequentially, the nanodots in the H2 thin film are erasable.

Our experiments show clearly the erasable and rewritable nanorecording behaviors in H2 thin films as a result of the conductance transition in the H2 rotaxane molecules. This work indicates the potential for the chemical modification of the rotaxane molecules as a promising route toward molecular memories, which have stable electrical properties and a long lifetime suitable for practical applications.

Acknowledgment. We thank Lifeng Chi, Harald Fuchs at Muenster University in Germany, and Zhihai Cheng and Xiao Lin for experimental assistance. Work at IOP was supported by grants from National Science Foundation of China, National “863” and “973” projects of China, the Chinese Academy of Sciences, and Supercomputing Center, CNIC, CAS.

References

- (1) Gao, H. J.; Xue, Z. Q.; Wang, K. Z.; Wu, Q. D.; Pang, S. J. *Appl. Phys. Lett.* **1996**, *68*, 2192–2194.
- (2) Shi, D. X.; Song, Y. L.; Zhang, H. X.; Jiang, P.; He, S. T.; Xie, S. S.; Pang, S. J.; Gao, H. J. *Appl. Phys. Lett.* **2000**, *77*, 3203–3205.
- (3) Shi, D. X.; Song, Y. L.; Zhang, H. X.; Jiang, P.; Xie, S. S.; Pang, S. J.; Gao, H. J. *Adv. Mater.* **2001**, *13*, 1103–1105.
- (4) Gao, H. J.; Sohlberg, K.; Xue, Z. Q.; Chen, H. Y.; Hou, S. M.; Ma, L. P.; Fang, X. W.; Pang, S. J.; Pennycook, S. J. *Phys. Rev. Lett.* **2000**, *84*, 1780–1783.
- (5) Wu, H. M.; Song, Y. L.; Du, S. X.; Liu, H. W.; Gao, H. J.; Jiang, L.; Zhu, D. B. *Adv. Mater.* **2003**, *15*, 1925–1929.
- (6) Wen, Y. Q.; Song, Y. L.; Jiang, G. Y.; Zhao, D. B.; Ding, K. L.; Yuan, W. F.; Lin, X.; Gao, H. J.; Jiang, L.; Zhu, D. B. *Adv. Mater.* **2004**, *16*, 2018–2021.
- (7) Norgaard, K.; Laursen, B. W.; Nygaard, S.; Kjaer, K.; Tseng, H.-R.; Flood, A. H.; Stoddart, J. F.; Bjornholm, T. *Angew. Chem., Int. Ed.* **2005**, *44*, 7035–7039.
- (8) Jang, S. S.; Jang, Y. H.; Kim, Y.-H.; Goddard, W. A., III; Choi, J. W.; Heath, J. R.; Laursen, B. W.; Flood, A. H.; Stoddart, J. F.; Norgaard, K.; Bjornholm, T. *J. Am. Chem. Soc.* **2005**, *127*, 14804–14816.
- (9) Feng, M.; Guo, X. F.; Lin, X.; He, X. B.; Ji, W.; Du, S. X.; Zhang, D. Q.; Zhu, D. B.; Gao, H. J. *J. Am. Chem. Soc.* **2005**, *127*, 15338–15339.
- (10) Guo, X. F.; Zhou, Y. C.; Feng, M.; Xu, Y.; Zhang, D. Q.; Gao, H. J.; Fan, Q. H.; Zhu, D. B. *Adv. Func. Mater.* **2007**, in press.
- (11) Jang, Y. H.; Hwang, S.; Kim, Y.-H.; Jang, S. S.; Goddard, W. A., III. *J. Am. Chem. Soc.* **2004**, *126*, 12636–12645.
- (12) Deng, W.-Q.; Muller, R. P.; Goddard, W. A., III. *J. Am. Chem. Soc.* **2004**, *126*, 13562–13563.
- (13) Kim, Y. H.; Jang, S. S.; Jang, Y.-H.; Goddard, W. A., III. *Phys. Rev. Lett.* **2005**, *94*, 156801–1–4.

JA067037P